

Little Red Dots and Supermassive Black Hole Seed Formation in Ultralight Dark Matter Halos

Dongsu Bak*

Physics Department, University of Seoul, Seoul, 02504, Korea

Jae-Weon Lee†

*Department of Electrical and Electronic Engineering,
Jungwon University, 85 Munmu-ro, Goesan-eup,
Goesan-gun, Chungcheongbuk-do, 28024, Korea.*

We investigate how supermassive black hole (SMBH) seeds form in the early Universe at the centers of ultralight dark matter (ULDM) halos. Focusing on the ULDM Jeans scale, we identify the critical conditions under which high-redshift baryonic gas, strongly confined by central solitonic cores of the halos, undergoes direct and monolithic collapse. The solitonic potential naturally drives rapid inflow and shock heating, allowing the gas temperature to exceed the critical atomic-cooling threshold of $\sim 10^4$ K required for fragmentation suppression without invoking an external UV background. We derive semi-analytic relations for the halo mass, soliton mass, baryonic core radius, and thermodynamic state of the gas, including the effects of baryonic contraction. These relations simultaneously determine the minimum and maximum SMBH seed masses as functions of redshift. In this framework, pristine gas clouds that satisfy the temperature threshold collapse without fragmentation, forming SMBH seeds with characteristic masses of order $10^5 M_\odot$, while systems below the threshold are expected to form compact star clusters instead. Our model also implies an upper limit on the attainable SMBH mass, predicting a maximum mass scale of order $10^{10} M_\odot$, consistent with the most massive quasars observed to date. The ULDM particle mass required to reproduce the inferred seed mass scale, $m \simeq 10^{-22}$ eV, coincides with the value favored by galactic-scale observations, providing a unified explanation for the characteristic masses of both galactic cores and early SMBH seeds. Our model predicts efficient SMBH seed formation at redshifts $z \gtrsim 10$ and offers a natural interpretation of recently observed little red dots as SMBHs embedded in compact, hot, ionized gas clouds.

I. INTRODUCTION

The detection of bright quasars less than a billion years after the Big Bang indicates that supermassive black holes (SMBHs) with masses up to $\sim 10^9 M_\odot$ already existed at the redshifts $z \gtrsim 6$, posing a serious challenge to models of black hole seeding and early growth [1, 2]. In stellar-remnant seed scenarios, maintaining nearly continuous and efficient accretion is difficult in shallow potential wells at high redshift, which motivates massive-seed scenarios where black holes are born with initial masses of $\sim 10^4$ – $10^6 M_\odot$ [1–3].

The direct-collapse black hole (DCBH) scenario assumes that a primordial, metal-free gas cloud undergoes an almost monolithic collapse to form a supermassive star or a quasi-star which subsequently gives rise to a massive black hole seed [4, 5]. The key requirement for this scenario is the suppression of

*Electronic address: dsbak@uos.ac.kr

†Electronic address: scikid@jwu.ac.kr

fragmentation, which could be achieved by maintaining the gas temperature at $\sim 10^4$ K and preventing efficient molecular hydrogen cooling, often via a strong Lyman-Werner UV background or dynamical heating [2, 6–8]. Recent observations of little red dots (LRDs) [9] indicate that black hole seeds with masses $M_{bh} \gtrsim 10^5 M_\odot$ formed at the centers of compact, hot, ionized, pristine gas clouds in the early Universe. It is noteworthy that the observed minimum mass of these seeds is comparable to the characteristic minimum mass of galactic cores $\sim 10^6 M_\odot$ [10]. It is therefore tempting to speculate that these two mass scales are physically connected.

One possible explanation for the characteristic mass scale of galactic cores [11] is ultralight dark matter (ULDM) [12–22], which has been extensively studied as an alternative to cold dark matter (CDM) and may alleviate small-scale issues of CDM such as the cusp problem. In this model, dark matter consists of extremely light scalar particles with mass $m \simeq 10^{-22} eV$ whose macroscopic de Broglie wavelength leads to quantum pressure supported cores (solitons) embedded in larger halos [21, 23, 24]. These solitonic cores typically have masses $M_{sol} \gtrsim 10^6 M_\odot$ and provide deep, centrally concentrated gravitational potentials that can significantly boost baryonic collapse at high redshift [25], while also helping to alleviate the final parsec problem [26, 27].

In this paper, we explore ULDM-assisted SMBH seed formation in which the solitonic core acts as a deep potential well for direct collapse of baryon clouds. The key idea is that baryons gravitationally confined within the soliton can undergo rapid infall accompanied by strong shock heating, thereby driving the gas into a regime where molecular cooling becomes dynamically subdominant, even without invoking an external UV background. We develop semi-analytic scalings for (i) the characteristic halo and soliton properties as functions of the ULDM mass m and redshift z , and (ii) the thermodynamic state of baryons collapsing inside the soliton potential. By applying the zone-of-no-return criterion for the suppression of H_2 cooling [28], we identify the parameter regime in which fragmentation is avoided and global collapse can occur [2–4, 29]. In this way, the ULDM soliton provides a natural, purely gravitational route to sustained high inflow rates and elevated temperatures, enabling the formation of supermassive stars with characteristic masses $\sim 10^5 M_\odot$ that can rapidly evolve into SMBH seeds consistent with high-redshift quasar and LRD observations [1, 2, 5, 30].

Section II summarizes the ULDM quantum Jeans scales for halos and the soliton-halo relations used in this work. Section III derives the baryonic core properties inside ULDM solitons and applies the zone-of-no-return criterion for H_2 cooling suppression to determine the fragmentation suppression conditions and the resulting seed mass scale. Section IV discusses the broader implications of our model for early structure formation, including its physical interpretation of LRDs, the observational consequences and limitations of the scenario.

II. JEANS LENGTH AND HALO MASS FUNCTION OF ULTRALIGHT DARK MATTER

In this section, we present the characteristic scales that determine early halos and the corresponding central solitons. The quantum Jeans length scale is given by

$$\lambda_J(z) = \frac{\pi^{3/4} \hbar^{1/2}}{(G\rho(z))^{1/4} m^{1/2}} = 9.217 \times 10^4 (1+z)^{-3/4} m_{22}^{-1/2} \left(\frac{0.27}{\Omega_{\text{dm}}}\right)^{1/4} \left(\frac{0.7}{h}\right)^{1/2} \text{ pc}, \quad (\text{II.1})$$

where $m_{22} \equiv m/10^{-22} eV$, h is the reduced Hubble constant, and Ω_{dm} is the dark matter density parameter. The dark matter density at redshift z is

$$\rho_{\text{dm}}(z) = \rho_{\text{dm}}(0) (1+z)^3. \quad (\text{II.2})$$

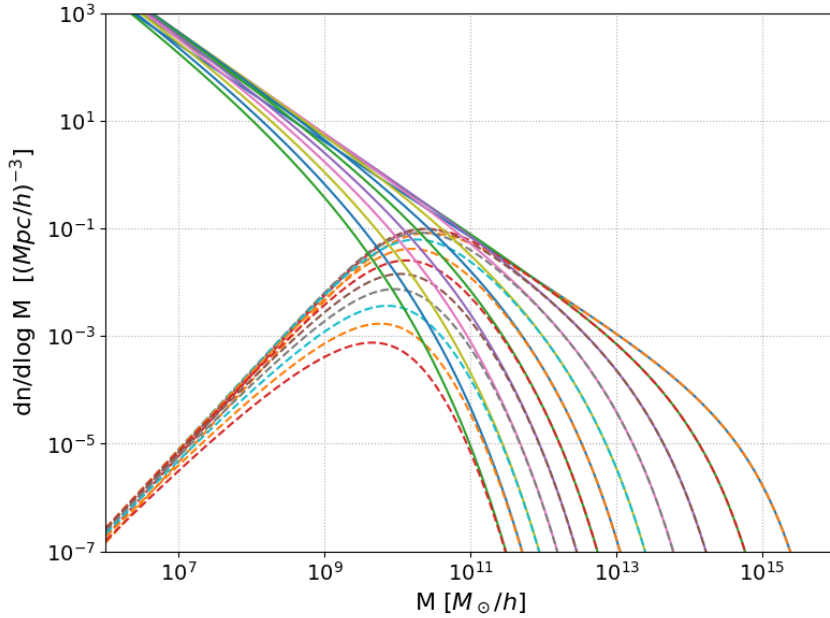


FIG. 1: Halo mass functions (HMFs) for CDM (solid lines) and ULDM (dashed lines, for $m_{22} = 1$) at redshifts $z = 0 \sim 11$, computed within the Press-Schechter formalism. HMFs increase as z decreases, with the highest curves corresponding to $z = 0$. Relative to CDM, ULDM shows a pronounced suppression of low-mass halos arising from the small-scale cutoff in the matter power spectrum.

The quantum Jeans mass scale is then defined by [11, 19, 31]

$$M_J(z) = \frac{4\pi}{3} \rho_{dm}(z) \lambda_J^3(z) = 1.204 \times 10^8 \left(\frac{1+z}{m_{22}^2} \right)^{3/4} \left(\frac{\Omega_{dm}}{0.27} \right)^{1/4} \left(\frac{h}{0.7} \right)^{1/2} M_\odot, \quad (\text{II.3})$$

which implies that ULDM halos can provide sufficiently deep potential wells to confine baryons at high redshift. The dark matter halo mass must satisfy $M_h \geq M_J$, since a radius λ of a ULDM perturbation is constrained by $\lambda \geq \lambda_J$. Halo collapse occurs only in the mass range $M_{\text{upper}} \geq M_h \geq M_J$. The upper bound M_{upper} reflects the observed number density of galactic halos.

We shall assume $\Omega_{dm} = 0.27$ and $h = 0.7$ in this paper. Then, the dark matter density at the redshift z is given by

$$\rho_{dm}(z) = 0.2485 \times 10^{-29} (1+z)^3 \text{g/cm}^3. \quad (\text{II.4})$$

Taking $M_h \equiv \alpha^3 M_J$, the collapse condition becomes $\alpha_{max}(z) \geq \alpha \geq 1$ where

$$\alpha_{max}(z) \equiv \left(\frac{M_{\text{upper}}(z)}{M_J} \right)^{1/3}. \quad (\text{II.5})$$

This leads to the halo mass as a function of the parameter α

$$M_h = \frac{4\pi}{3} \rho(z) \alpha^3 \lambda_J^3(z) = 1.204 \times 10^8 \alpha^3 \left(\frac{1+z}{m_{22}^2} \right)^{3/4} M_\odot. \quad (\text{II.6})$$

To obtain M_{sol} from the halo mass one may use the empirical formula for the core-halo relation for ULDM [32]

$$M_{sol} = 1.680 \times 10^9 m_{22}^{-1} \frac{\xi'(z)}{\xi'(7)} \left(\frac{M_h}{10^{11} M_\odot} \right)^{1/3} M_\odot, \quad (\text{II.7})$$

where $\xi'(z) = \sqrt{1+z}\xi(z)^{1/6}$ and $\xi(z) = (18\pi^2 + 82(\Omega_m(z) - 1) - 39(\Omega_m(z) - 1)^2)/\Omega_m(z) \simeq 177$ for $\frac{4}{3}$ large z . When $z > 7$ (or even $z > 1$), the relative change in $\xi(z)$ can be ignored. Using the halo mass as given above, the core soliton mass becomes

$$M_{sol} = 0.6319 \times 10^8 \alpha \left(\frac{1+z}{m_{22}^2} \right)^{3/4} M_{\odot}. \quad (\text{II.8})$$

The corresponding half-mass radius of the soliton is given by

$$r_{1/2} = \frac{2\beta f_0}{3} \frac{\hbar^2}{m^2} \frac{1}{GM_{sol}} = 3.539 \frac{\beta}{m_{22}^2 \alpha} \left(\frac{1+z}{m_{22}^2} \right)^{-3/4} \text{ kpc} \quad (\text{II.9})$$

with $f_0 = 3.9251$ [24]. We insert here an extra factor $2\beta/3$ to account for the reduction of the half-mass radius due to the presence of the baryonic matter. This factor β is expected to be of order unity, and we set $\beta = 1$ below for simplicity. To reproduce the observed galactic core sizes, we require $r_{1/2} \simeq \text{kpc}$, which corresponds to $m \simeq 10^{-22} \text{eV}$ [33]. Interestingly, the average dark matter density at the half mass radius

$$\rho_{1/2} = \frac{3M_{sol}}{8\pi r_{1/2}^3} = 1.152 \times 10^{-26} \alpha^4 (1+z)^3 \text{g/cm}^3 = 1.702 \times 10^{-4} \alpha^4 (1+z)^3 M_{\odot}/\text{pc}^3 \quad (\text{II.10})$$

becomes independent of m . One finds that compared to the CDM model ULDM halos at redshift z can develop extremely compact and high-density cores, particularly in systems hosting massive solitons with large M_{sol} .

In this study, the halo mass function (HMF) is required to link the theoretically allowed collapse window to the cosmological abundance of host halos, thereby enabling a direct assessment of whether the proposed seed-formation conditions can account for the observed population of SMBHs. We adopt the Press–Schechter (PS) formalism [34], which gives

$$\frac{dn}{d \ln M} = -\frac{1}{2} \frac{\rho_0}{M} f(\nu) \frac{d \ln \sigma^2}{d \ln M}, \quad (\text{II.11})$$

where $\nu \equiv \frac{\delta_c}{\sigma}$ with the critical overdensity δ_c , and dn is the abundance of halos within a mass interval dM . For CDM, we adopt the Sheth-Tormen form for $f(\nu)$ [35] for simplicity:

$$f(\nu) = A \sqrt{\frac{2}{\pi}} \sqrt{q\nu} \left(1 + (q\nu)^{-2p} \right) \exp \left[-\frac{q\nu^2}{2} \right] \quad (\text{II.12})$$

with parameters $\{A = 0.3222, p = 0.3, q = 0.707\}$. Compared to the CDM case, the HMF for ULDM is suppressed at low masses as a result of the quantum pressure-induced cutoff in the matter power spectrum as [36]

$$\left. \frac{dn}{d \ln M} \right|_{\text{ULDM}} = \left. \frac{dn}{d \ln M} \right|_{\text{CDM}} \left[1 + \left(\frac{M_h}{M_0} \right)^{-1.1} \right]^{-2.2}, \quad (\text{II.13})$$

where $M_0 = 1.6 \times 10^{10} m_{22}^{-4/3} M_{\odot}$. Fig. 1 shows HMFs for CDM and ULDM at various redshifts z , computed within the PS formalism [37]. Relative to CDM, ULDM shows a pronounced suppression of low-mass halos.

To determine M_{upper} , one should integrate the HMF and compare the resulting abundance with observations. At a given redshift z , we define the maximum halo mass $M_{\text{upper}}(z)$ as the mass above which the expected number of halos within the observable Universe over the full sky is exactly unity. To determine this quantity, following Ref. [38], we numerically compute the cumulative comoving number

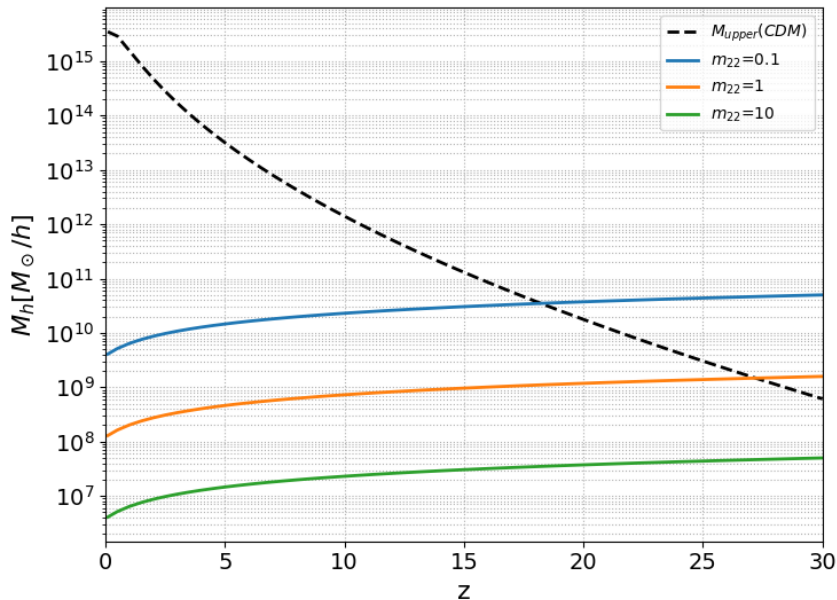


FIG. 2: The minimum mass M_J (the thick lines) and the maximum mass M_{upper} (the dashed line) of ULDM halos as functions of the redshift z for $m_{22} = (0.1, 1, 10)$, respectively. The halo mass decides the core masses of ULDM and those of gas clouds using the core-halo relation. For M_{upper} , we used the CDM approximation. At a given z , only halos with masses between M_J and M_{upper} can exist. Smaller m_{22} leads to later halo formation.

density $n(> M, z)$ from the Sheth–Tormen halo mass function. We then multiply this by the comoving volume element corresponding to a thin redshift slice $dz = 0.5$ over the full sky, to obtain the expected number of halos $N(> M, z)$. The maximum halo mass M_{upper} is defined by solving the condition $N(> M_{upper}(z), z) = 1$. This construction represents the mass of the most massive halo that is most likely to be observed near that redshift. For simplicity, we use the CDM halo mass function rather than the ULDM one to compute M_{upper} , which is a good approximation in the large M_h regime. We also assume that the minimum halo mass at z is set by the Jeans mass $M_J(z)$. With these assumptions, the minimum and maximum ULDM halo masses at a given z can be estimated. Then, from M_J and M_{upper} , one can obtain the ranges of α and M_{sol} using Eq. (II.7). Fig. 2 shows M_J and M_{upper} as functions of z for $m_{22} = (0.1, 1, 10)$, respectively. As z increases, M_{upper} decreases and the allowed range of M_h shrinks.

There is yet another upper bound for the soliton mass independent of z . The maximum gravitationally stable mass of an isolated ground-state configuration of ULDM is given by

$$M_{\max} \simeq 0.633 \frac{M_{\text{Pl}}^2}{m} \simeq \frac{8.5 \times 10^{11}}{m_{22}} M_{\odot}, \quad (\text{II.14})$$

where M_{Pl} is the Planck mass. A soliton with a mass exceeding this scale is unstable to gravitational cooling and tends to lose mass [39], unless it is compressed under extreme conditions such as high-speed collisions or in the very high-redshift Universe. Consequently, we expect the maximum dark matter core mass to be effectively bounded at approximately M_{\max} . This, in turn, may provide an upper bound on the masses of gas clouds within the core and on the ultimate masses of black holes formed and grown in the gas clouds. Note that M_{\max} is usually different from the soliton mass in halos with mass M_{upper} which is obtained from HMF.

We now consider baryons embedded within the dark matter soliton. In realistic collapse scenarios, atomic gas generically develops a finite-density isothermal core owing to shocks and efficient radiative cooling [40]. Therefore, a pseudo-isothermal profile

$$\rho_b(r) = \frac{\rho_0}{1 + r^2/r_c^2} \quad (\text{III.1})$$

is the physically relevant description for the gas cloud [41], where ρ_0 is the central density and r_c is the core radius of the gas cloud. For the pseudo-isothermal profile adopted in this work, the baryon mass up to radius r is given by

$$M_b(r) = 4\pi\rho_0 r_c^3 \left(\frac{r}{r_c} - \arctan \frac{r}{r_c} \right) = 4\pi\rho_0 r_c^3 G \left(\frac{r}{r_c} \right), \quad (\text{III.2})$$

where $G(x) \equiv x - \arctan(x)$. We adopt this mass profile for initial gas distribution within the ULDM cores. The concentration parameter for the pseudo-isothermal profile $c_r \equiv r_{vir}/r_c$ is typically about 30 [42], where r_{vir} is the virial radius of the gas clouds. Since we expect baryons to collapse into the gravitational potential well of ULDM soliton cores, for simplicity, we assume r_{vir} is equal to the half-mass radius $r_{1/2}$ of the ULDM soliton cores. Then, $M_b(r_{vir}) \simeq 0.2M_{sol}/2 \simeq 4\pi\rho_0 r_c^3 G(r_{vir}/r_c)$, where 0.2 represents the approximate mass ratio of baryon to dark matter.

From Eq. (II.9), the baryonic core radius becomes

$$r_c = r_{1/2}/c_r \simeq 118.0 \times \frac{1}{\alpha m_{22}^2} \left(\frac{1+z}{m_{22}^2} \right)^{-3/4} \text{pc} \quad (\text{III.3})$$

for $c_r = 30$. Then, one can obtain

$$M_b(r) \simeq \frac{0.1M_{sol}G\left(\frac{r}{r_c}\right)}{G(c_r)} \quad (\text{III.4})$$

and the baryon mass within the core

$$M_b(r_c) \simeq 4.764 \times 10^4 \alpha \left(\frac{1+z}{m_{22}^2} \right)^{3/4} M_\odot \quad (\text{III.5})$$

using Eq. (II.8). The average baryon density at the radius r_c becomes

$$\rho_b(r_c) \simeq \frac{3M_b(r_c)}{4\pi r_c^3} \simeq 6.929 \times 10^{-3} \alpha^4 (1+z)^3 M_\odot/\text{pc}^3. \quad (\text{III.6})$$

We shall take this gas cloud with $r \leq r_c$ as the initial baryonic core that undergoes subsequent collapse via the Jeans instability. Therefore, r_c represents the initial size of the baryonic core that undergoes direct collapse. As the collapse proceeds, the core contracts to smaller radii and its baryon density increases beyond the value given in the above equation. The ULDM density at $r = r_c$ is much lower than the baryon density and ULDM mass and its gravitational contribution may be ignored once the gas core is formed.

The Jeans scale of ULDM determines the minimum halo mass able to collapse at high redshift, while the empirical soliton-halo relation fixes the soliton mass and dark matter core radius. These, in turn, set the baryonic core density, inflow velocity, shock temperature, and accretion rate.

The mass of the seed black hole may be expressed as

$$M_{bh} = f_{bh} M_b(r_c), \quad (\text{III.7})$$

where we adopt a value $f_{bh} \simeq O(0.1)$, motivated by the fact that M_{bh} can grow to as much as about half of the quasi-star mass [43, 44]. Therefore, the mass of the black hole seeds formed at z may satisfy

$$4.764 f_{bh} \times 10^4 \left(\frac{1+z}{m_{22}^2} \right)^{3/4} M_{\odot} \lesssim M_{bh} \lesssim 4.764 f_{bh} \times 10^4 \alpha_{max} \left(\frac{1+z}{m_{22}^2} \right)^{3/4} M_{\odot}, \quad (\text{III.8})$$

where α_{max} can be inferred from M_{upper} . However, we will show that not all seeds within this mass range can form if the temperature of the gas is not sufficiently high. (See Eq. (III.22) below.)

One can also estimate the maximum mass of SMBHs grown from their seeds. If we assume that a seed forms and grows within the most massive physically allowed soliton (i.e., $M_{sol} \simeq M_{max}$) and consumes all remaining baryonic mass enclosed within the core, then its mass can be as large as $0.2 f_{bh} M_{max}$. This sets the characteristic mass scale of the most massive SMBHs (not just seeds),

$$M_{bh}^{max} \equiv 0.2 f_{bh} M_{max} \simeq \frac{1.7 \times 10^{11} f_{bh}}{m_{22}} M_{\odot}. \quad (\text{III.9})$$

Interestingly, from the observational data $M_{bh}^{max} \simeq 10^{10} M_{\odot}$ [2], one again obtains $m \simeq 10^{-22} eV$ for $f_{bh} = 0.1$. Because such massive solitons and the corresponding SMBHs are rare, mergers among them are expected to be infrequent. Consequently, this mass scale is not expected to change significantly due to mergers in cosmic history (see Fig. 3).

We now estimate the shock temperature of the core gas cloud as

$$T_{core} \simeq \frac{3\mu m_H}{16k_B} v_{in}^2 \simeq \frac{3\mu m_H}{8k_B} \frac{GM_b(r_c)}{r_c}, \quad (\text{III.10})$$

where $v_{in} \equiv \sqrt{2GM_b(r_c)/r_c}$ denotes the gas inflow velocity, m_H is the hydrogen mass, and we take $\mu = 1.0$ for definiteness. This leads to

$$T_{core} \simeq 78.96 (1+z)^{\frac{3}{2}} \frac{\alpha^2}{m_{22}} \text{K}, \quad (\text{III.11})$$

which can easily exceed 10^3K for $z > 10$ and $\alpha \gg 1$.

From Eq. (III.6) one can obtain the number density of hydrogen atoms in the initial core

$$n_H \simeq 0.2803 \alpha^4 (1+z)^3 / \text{cm}^3. \quad (\text{III.12})$$

These satisfy the relation

$$T_{core} / n_H^{1/2} = q' / m_{22} \text{Kcm}^{3/2} \quad (\text{III.13})$$

with $q' = 78.96 / 0.2803^{1/2} \simeq 149.2$. For concreteness, in this paper we assume the direct collapse scenario in the reference 28, where H_2 is collisionally dissociated and molecular cooling is suppressed. The gas remains on the efficient atomic cooling track at the temperature $T \simeq 8000 \text{K}$ and undergoes a nearly isothermal collapse, avoiding fragmentation and leading to the formation of a supermassive star, which can subsequently collapse into a black hole. From Eq. (9) and Eq. (10) of Ref. 28, the the zone of no-return condition for direct collapse can be summarized as

$$T_{core} n_H \geq q_l \text{K/cm}^3 \quad \text{and} \quad T_{core} n_H^{0.1} \geq q_r \text{K/cm}^{0.3}, \quad (\text{III.14})$$

where $q_l = 0.56 \times 10^8$ and $q_r = 0.5 \times \sqrt{10} \times 10^4 = 1.581 \times 10^4$. The two boundary lines meet at $T = (q_r^{10}/q_l)^{1/9} \text{K} = 0.6377 \times 10^4 \text{K}$ and $n_H = (q_l/q_r)^{10/9} / \text{cm}^3 = 0.8782 \times 10^4 / \text{cm}^3$. If the initial values

of T_{core} and n_H lie within the zone of no return, the direct collapse begins. Hence the direct collapse conditions are satisfied if

$$\begin{aligned} T_{core} &\geq (q_l(q'/m_{22})^2)^{1/3}K = 1.076 \times 10^4 \text{ K}/m_{22}^{2/3} \text{ and} \\ T_{core} &\geq (q_r^5 q'/m_{22})^{1/6}K = 0.7268 \times 10^4 \text{ K}/m_{22}^{1/6}. \end{aligned} \quad (\text{III.15})$$

As both bounds are functions of m_{22} , only the larger of the two needs to be satisfied. The two lower bound temperatures become the same if $m_{22} = q' q_l^{2/3}/q_r^{5/3} \equiv a_0 = 2.192$. Therefore, there are two cases.

If $m_{22} \leq a_0 = 2.192$, the collapse condition becomes $T_{core} \geq (q_l(q'/m_{22})^2)^{1/3}K$. The threshold core temperature is of order 10^4 K , which is high enough to dissociate H_2 . In this case, from Eq. (III.11) direct collapse becomes possible if

$$\alpha^2 \frac{(1+z)^{3/2}}{m_{22}^{1/3}} \gtrsim (q_l q'^2)^{1/3}/78.96 = 136.3 \quad (\text{III.16})$$

or

$$\alpha \gtrsim \alpha_{th} = (q_l q'^2)^{1/6}/\sqrt{78.96} \times \frac{m_{22}^{1/6}}{(1+z)^{3/4}} = 11.67 \times \frac{m_{22}^{1/6}}{(1+z)^{3/4}} \quad (\text{III.17})$$

which leads to

$$M_b(r_c)|_{\alpha=\alpha_{th}} = 4.764 \times 10^4 \times (q_l q'^2)^{1/6}/\sqrt{78.96} \times m_{22}^{-4/3} M_\odot = 0.5562 \times 10^6 \times m_{22}^{-4/3} M_\odot. \quad (\text{III.18})$$

Then, here and below, the minimum seed mass is given by

$$M_{bh}^{min} \equiv f_{bh} M_b(r_c)|_{\alpha=\alpha_{th}}. \quad (\text{III.19})$$

On the other hand, if $m_{22} \geq a_0$, the collapse condition becomes $T_{core} \geq (q_r^5 q'/m_{22})^{1/6}K$. In this case direct collapse becomes possible if

$$\alpha^2 \frac{(1+z)^{3/2}}{m_{22}^{5/6}} \gtrsim (q_r^5 q')^{1/6}/78.96 = 92.04 \quad (\text{III.20})$$

or

$$\alpha \gtrsim \alpha_{th} = (q_r^5 q')^{1/12}/\sqrt{78.96} \times \frac{m_{22}^{5/12}}{(1+z)^{3/4}} = 9.594 \times \frac{m_{22}^{5/12}}{(1+z)^{3/4}} \quad (\text{III.21})$$

which leads to

$$M_b(r_c)|_{\alpha=\alpha_{th}} = 4.764 \times 10^4 \times (q_r^5 q')^{1/12}/\sqrt{78.96} \times m_{22}^{-13/12} M_\odot = 0.4571 \times 10^6 \times m_{22}^{-13/12} M_\odot. \quad (\text{III.22})$$

Combining these results with the observational constraint for the minimum seed mass $10^4 M_\odot \lesssim M_{bh}^{min} \lesssim 10^5 M_\odot$ yields interesting bounds for the particle mass of ULDM

$$3.622 f_{bh}^{3/4} \lesssim m_{22} \lesssim 20.37 f_{bh}^{3/4}, \quad (\text{III.23})$$

for the case 1 and

$$4.067 f_{bh}^{12/13} \lesssim m_{22} \lesssim 34.07 f_{bh}^{12/13}, \quad (\text{III.24})$$

for the case 2, which are consistent with the ULDM particle mass $m \simeq O(10^{-22})eV$ inferred from galactic dynamics for $f_{bh} \simeq O(0.1)$. For $m \gg 10^{-22}eV$, SMBH seeds are too small in mass, whereas for

$m \ll 10^{-22} eV$ their masses are excessively large and the seeds form too late (see Fig. 2). Interestingly,⁹ ULDM with the fiducial mass $m \simeq 10^{-22} eV$ seems to explain the minimum mass and the maximum mass of observed SMBHs. (See Fig. 3.) Cores of gas clouds with masses below the threshold given in Eq. (III.18) and in Eq. (III.22) fail to form black hole seeds and instead are expected to form star clusters.

Our model suggests the possible existence of LRDs. After SMBH seeds form inside the baryonic core, the remaining hot gas forms a cocoon surrounding the seeds. Let us consider the case 1 ($m_{22} \leq 2.192$) for example. From Eq. (III.17) and Eq. (III.3), one finds that the initial baryonic core size is smaller than

$$r_c|_{\alpha=\alpha_{th}} = 10.11 m_{22}^{-2/3} \text{pc}, \quad (\text{III.25})$$

and the radius of the whole gas cloud is smaller than

$$r_{vir}|_{\alpha=\alpha_{th}} = c_r r_c|_{\alpha=\alpha_{th}} \simeq 303.3 m_{22}^{-2/3} \text{pc}, \quad (\text{III.26})$$

which is consistent with LRD observations [45] implying an effective radius of gas clouds ~ 100 pc.

From Eq. (III.3) and Eq. (III.5), the mass inflow rate $\dot{M} = 4\pi r_c^2 \rho_b(r_c) v_{in} = 3\sqrt{2G} M_b(r_c)^{3/2} / r_c^{3/2}$ is given by

$$\dot{M} \simeq 2.308 \times 10^{-3} \alpha^3 m_{22}^{-3/2} (1+z)^{9/4} M_\odot/\text{yr} > 3.669 m_{22}^{-1} M_\odot/\text{yr}, \quad (\text{III.27})$$

where we used the bound $\alpha > \alpha_{th}$ of the case 1 for the last inequality. This strong inflow ($\dot{M} \gg 0.1 M_\odot/\text{yr}$) further ensures that the gas collapses monolithically to form a massive protostellar core [46], providing a dynamical pathway to SMBH seeds. Once SMBH seeds form, ULDM solitons can supply additional gravitational potential that enhances the Bondi accretion rate onto a growing black hole seed [25], thereby enhancing the growth of SMBHs. Note that we do not consider angular momentum transfer and radiation feedback here, for simplicity.

In our model, SMBH seeds can form at high $z > 10$, possibly alleviating the tension of the standard scenario of black hole formation. Assuming Eddington-limited accretion with a radiative efficiency of $\epsilon = 0.1$, the black hole mass evolves as [53]

$$M(z_f) = M_i \exp \left[\frac{t(z_f) - t(z_i)}{t_{\text{Sal}}} \right], \quad (\text{III.28})$$

where $t_{\text{Sal}} \simeq 45$ Myr is the Salpeter e-folding timescale. For example, for the quasar in the galaxy UHZ1 with mass $M(z_f) = 4 \times 10^7 M_\odot$ at $z_f = 10.1$ [52], starting from an initial seed mass $M_i = 10^5 M_\odot$, the required growth factor is $M(z_f)/M_i = 400$. This implies $t(z_f) - t(z_i) \simeq 2.7 \times 10^8 \text{yr}$, which corresponds to an initial redshift $z_i \simeq 19$. (See Fig. 3.) Therefore, a heavy seed of mass $10^5 M_\odot$ in our scenario can naturally grow to $\sim 4 \times 10^7 M_\odot$ by $z \simeq 10$, demonstrating that early SMBH growth is feasible without invoking super-Eddington accretion. Fig. 3 shows the mass spectrum of observed quasars and candidate SMBHs in LRDs, which is well reproduced by our theoretical predictions. Our model predicts that many LRDs with SMBHs having masses $M_{bh} \gtrsim 10^5 M_\odot$ exist even beyond $z > 7$.

IV. DISCUSSION

Observations of LRDs indicate that black hole seeds with masses $M_{bh} \gtrsim 10^5 M_\odot$ already exist at $z \gtrsim 5$, and our scenario provides a physical interpretation of their origin. In this work, we show that this characteristic mass scale arises naturally in the ULDM scenario: when the baryonic core inside a soliton satisfies the temperature threshold, the enclosed gas mass reaches $M_b(r_c)|_{\alpha=\alpha_{th}} \sim 10^6 M_\odot$, and a fraction $f_{bh} \sim 0.1$ of this mass is converted into a black hole, yielding a seed of order $10^5 M_\odot$ without fine-tuning.

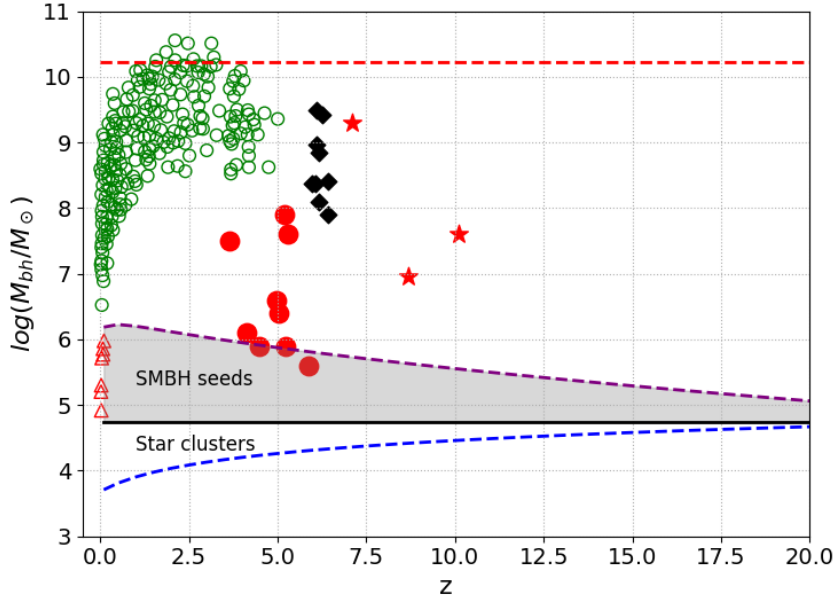


FIG. 3: The mass spectrum of SMBHs as a function of redshift. The black horizontal line denotes the minimum masses of SMBH seeds M_{bh}^{min} given in Eq. (III.19) corresponding to α_{th} . We choose $m = 10^{-22} eV$ and $f_{bh} = 0.1$ here. The blue dashed line and the purple dashed line denote the possible SMBH seed mass in Eq. (III.8) for $\alpha = 1$ and $\alpha = \alpha_{max}$, respectively. However, objects located between the black horizontal line and the blue line cannot be genuine black hole seeds because the gas temperature is too low and fragmentation is unavoidable; instead, these systems are expected to form star clusters. According to Eq. (III.18) in our model, only gas clouds corresponding to the SMBH seeds in the gray region possess sufficient self-gravity and temperature to form a SMBH seed. The dashed horizontal red line denotes the maximum black hole mass M_{bh}^{max} in Eq. (III.9) set by the stability of the soliton. Dots represent the observed masses of SMBHs from various observations [47–52]. The red triangles denote XMM-Newton observations [47], the green circles represent LBQS observations [48], the black diamonds denote CFHQS observations [49]. The red stars denote quasars with $z > 7$ [50–52], while the red star at $z = 10.1$ is for the quasar in the galaxy UHZ1. The red disks denote the candidate SMBHs in LRDs [9].

A key outcome of this work is that the typical seed mass is not an ad hoc assumption but instead follows from the intrinsic mass and length scales set by ULDM.

The deep gravitational potential of the soliton also leads to rapid gas inflow and shock heating up to $T_{core} \sim 10^4$ K, suppressing molecular hydrogen cooling and preventing fragmentation, consistent with the compact, hot, and ionized environments inferred for LRDs. Below the threshold mass, gas clouds generically fail to form black hole seeds and are instead expected to collapse into dense star clusters, possibly accounting for the observed coexistence of AGN-like and young stellar-dominated LRDs [54], and potentially triggering the early formation of galaxies within a single physical framework. Furthermore, because the relevant Jeans scale and the soliton–halo relation favor the formation of dense cores at high redshift, our scenario predicts that SMBH seed formation is efficient even at $z \geq 10$, explaining the early redshift range where LRDs are observed by JWST. Finally, we demonstrate that standard Eddington-limited accretion is sufficient to grow these seeds to the observed SMBH masses by $z \sim 10$, without invoking super-Eddington accretion.

This mechanism has several important implications for early structure formation. It provides a new connection between the small-scale physics of ULDM and the early growth of supermassive black holes, suggesting that the existence and typical masses of high-redshift SMBHs may carry indirect information

about ULDM particle properties. At the same time, the scenario makes testable predictions for the host halo masses, event rates, and thermodynamic conditions of early black hole formation, which can be confronted with upcoming observations of the high-redshift Universe. For example, our model predicts a substantial population of LRDs hosting SMBHs with masses $M_{bh} \gtrsim 10^5 M_\odot$ at redshifts $z > 7$.

The effects of angular momentum and radiative feedback are not included in the present semi-analytic treatment, although the solitonic potential is expected to promote rapid infall. While our model qualitatively reproduces key properties inferred for LRDs and SMBHs, including the characteristic mass scale, formation epoch, and the presence of hot, ionized gas, a more quantitative comparison with their number density and host-halo properties is still needed. While the Press–Schechter approach provides a useful estimate, more accurate ULDM halo mass functions derived from simulations should be explored in future work. Addressing these issues will require high-resolution simulations [40] and improved observational constraints, and the present work should therefore be regarded as a starting point for more detailed studies linking the small-scale physics of ULDM to the observed population of high-redshift SMBHs.

Acknowledgments

DB was supported in part by Basic Science Research Program through NRF funded by the Ministry of Education (2018R1A6A1A06024977).

-
- [1] M. Volonteri, *The Astronomy and Astrophysics Review* **18**, 279 (2010), 1003.4404.
 - [2] K. Inayoshi, E. Visbal, and Z. Haiman, *Annual Review of Astronomy and Astrophysics* **58**, 27 (2020), 1911.05791.
 - [3] M. A. Latif and A. Ferrara, *Publications of the Astronomical Society of Australia* **33**, e051 (2016), 1605.07391.
 - [4] V. Bromm and A. Loeb, *The Astrophysical Journal* **596**, 34 (2003), astro-ph/0212400.
 - [5] M. C. Begelman, M. Volonteri, and M. J. Rees, *Monthly Notices of the Royal Astronomical Society* **370**, 289 (2006), astro-ph/0602363.
 - [6] J. A. Regan and M. G. Haehnelt, *Monthly Notices of the Royal Astronomical Society* **396**, 343 (2009), 0810.2802.
 - [7] C. Shang, G. L. Bryan, and Z. Haiman, *Monthly Notices of the Royal Astronomical Society* **402**, 1249 (2010), 0906.4773.
 - [8] E. Visbal, Z. Haiman, and G. L. Bryan, *Monthly Notices of the Royal Astronomical Society* **445**, 1056 (2014).
 - [9] V. Rusakov, D. Watson, G. P. Nikopoulos, et al., *Nature* **649**, 574 (2026).
 - [10] L. E. Strigari, J. S. Bullock, M. Kaplinghat, J. D. Simon, M. Geha, B. Willman, and M. G. Walker, *Nature* **454**, 1096 (2008), 0808.3772.
 - [11] J.-W. Lee, *Phys. Lett. B* **756**, 166 (2016), 1511.06611.
 - [12] M. R. Baldeschi, G. B. Gelmini, and R. Ruffini, *Physics Letters B* **122**, 221 (1983).
 - [13] S.-J. Sin, *Phys. Rev. D* **50**, 3650 (1994), hep-ph/9205208.
 - [14] J.-W. Lee and I.-G. Koh, *Phys. Rev. D* **53**, 2236 (1996), hep-ph/9507385.
 - [15] T. Matos and F. S. Guzman, *Class. Quant. Grav.* **17**, L9 (2000), gr-qc/9810028.
 - [16] W. Hu, R. Barkana, and A. Gruzinov, *Phys. Rev. Lett.* **85**, 1158 (2000), astro-ph/0003365.
 - [17] C. G. Boehmer and T. Harko, *Journal of Cosmology and Astroparticle Physics* **2007**, 025–025 (2007).
 - [18] P. H. Chavanis, *Astronomy and Astrophysics* **537**, A127 (2012).
 - [19] L. Hui, J. P. Ostriker, S. Tremaine, and E. Witten, *Phys. Rev. D* **95**, 043541 (2017), 1610.08297.
 - [20] T. Matos, L. A. Ureña-López, and J.-W. Lee, *Frontiers in Astronomy and Space Sciences* **11** (2024).
 - [21] E. G. M. Ferreira, *The Astronomy and Astrophysics Review* **29**, 7 (2021), 2005.03254.

- [22] D. J. E. Marsh, *Phys. Rep.* **643**, 1 (2016), 1510.07633.
- [23] H.-Y. Schive, T. Chiueh, and T. Broadhurst, *Nature Physics* **10**, 496 (2014), 1406.6586.
- [24] L. Hui, J. P. Ostriker, S. Tremaine, and E. Witten, *Physical Review D* **95**, 043541 (2017), 1610.08297.
- [25] H.-H. S. Chiu, H.-Y. Schive, H.-Y. K. Yang, H. Huang, and M. Gaspari, *Phys. Rev. Lett.* **134**, 051402 (2025).
- [26] H. Koo, D. Bak, I. Park, S. E. Hong, and J.-W. Lee, *Physics Letters B* **856**, 138908 (2024).
- [27] B. C. Bromley, P. Sandick, and B. Shams Es Haghi, *Phys. Rev. D* **110**, 023517 (2024).
- [28] K. Inayoshi and K. Omukai, *Monthly Notices of the Royal Astronomical Society* **422**, 2539–2546 (2012).
- [29] K. Omukai, *The Astrophysical Journal* **546**, 635 (2001), astro-ph/0011446.
- [30] S. Bhattacharya, D. Bose, B. Dasgupta, J. Doliya, and R. Laha (2025), 2512.23789.
- [31] M. Y. Khlopov, B. A. Malomed, I. B. Zeldovich, and Y. B. Zeldovich, *Mon. Not. Roy. Astron. Soc.* **215**, 575 (1985).
- [32] H. H. S. Chiu, H.-Y. Schive, H.-Y. K. Yang, H. Huang, and M. Gaspari, *Phys. Rev. Lett.* **134**, 051402 (2025), 2501.09098.
- [33] H.-Y. Schive, T. Chiueh, and T. Broadhurst, *Nature Phys.* **10**, 496 (2014), 1406.6586.
- [34] W. H. Press and P. Schechter, *Astrophys. J.* **187**, 425 (1974).
- [35] R. K. Sheth, H. J. Mo, and G. Tormen, *Mon. Not. Roy. Astron. Soc.* **323**, 1 (2001), astro-ph/9907024.
- [36] H.-Y. Schive, T. Chiueh, T. Broadhurst, and K.-W. Huang, *The Astrophysical Journal* **818**, 89 (2016).
- [37] S. Murray, C. Power, and A. Robotham (2013), 1306.6721.
- [38] I. Harrison and P. Coles, *Mon. Not. Roy. Astron. Soc.* **421**, L19 (2012), 1111.1184.
- [39] S. L. Liebling and C. Palenzuela, *Living Rev. Rel.* **26**, 1 (2023), 1202.5809.
- [40] S. J. Patrick, D. J. Whalen, M. A. Latif, and J. S. Elford, *Monthly Notices of the Royal Astronomical Society* **522**, 3795 (2023).
- [41] A. Trinca, A. Lupi, Z. Haiman, M. Volonteri, R. Valiante, R. Schneider, and R. Decarli (2026), 2601.14370.
- [42] P. R. Shapiro, I. T. Iliev, and A. C. Raga, *Monthly Notices of the Royal Astronomical Society* **307**, 203–224 (1999).
- [43] J. Hassan, R. Perna, M. Cantiello, P. Armitage, M. Begelman, and T. Ryu (2025), 2510.18301.
- [44] A. D. Santarelli, C. B. Campbell, E. Farag, E. P. Bellinger, P. Natarajan, and M. E. Caplan (2025), 2510.11772.
- [45] C. A. Guia, F. Pacucci, and D. D. Kocevski, *Research Notes of the AAS* **8**, 207 (2024), ISSN 2515-5172.
- [46] H. Umeda, T. Hosokawa, K. Omukai, and N. Yoshida, *The Astrophysical Journal Letters* **830**, L34 (2016).
- [47] G. C. Dewangan, S. Mathur, R. E. Griffiths, and A. R. Rao, *The Astrophysical Journal* **689**, 762 (2008).
- [48] M. Vestergaard and P. S. Osmer, *The Astrophysical Journal* **699**, 800–816 (2009).
- [49] C. J. Willott, L. Albert, D. Arzoumanian, J. Bergeron, D. Crampton, P. Delorme, J. B. Hutchings, A. Omont, C. Reylé, and D. Schade, *The Astronomical Journal* **140**, 546–560 (2010).
- [50] D. J. Mortlock, S. J. Warren, B. P. Venemans, M. Patel, P. C. Hewett, R. G. McMahon, C. Simpson, T. Theuns, E. A. González-Solares, A. Adamson, et al., *Nature* **474**, 616–619 (2011).
- [51] R. L. Larson, S. L. Finkelstein, D. D. Kocevski, T. A. Hutchison, J. R. Trump, P. Arrabal Haro, V. Bromm, N. J. Cleri, M. Dickinson, S. Fujimoto, et al., *The Astrophysical Journal Letters* **953**, L29 (2023).
- [52] P. Natarajan, F. Pacucci, A. Ricarte, A. Bogdan, A. D. Goulding, and N. Cappelluti (2023), 2308.02654.
- [53] J. W. Moffat (2020), 2011.13440.
- [54] M. Carranza-Escudero, C. J. Conselice, N. Adams, T. Harvey, D. Austin, P. Behroozi, L. Ferreira, K. Ormerod, Q. Duan, J. Trussler, et al., *The Astrophysical Journal Letters* **989**, L50 (2025).